

Efficient Use of Pilot Signals in Wideband CDMA Array-Receivers*

Sofiène AFFES, Nahi KANDIL, and Paul MERMELSTEIN

INRS-Télécommunications, Université du Québec

800, de la Gauchetière Ouest, Suite 6900, Montréal, Québec, H5A 1K6, Canada

Abstract— We extend application of a new scheme for efficient use of pilot signals in wideband CDMA array-receivers from the pilot-channel to the pilot-symbol case. The new scheme exploits the pilot signals for the simple resolution of the sign ambiguity arising in BPSK-decision-directed blind channel identification and achieves significant spectrum efficiency gains and power or overhead savings over the same array-receiver versions which use pilots for conventional channel identification only. Both analysis and simulations suggest that pilot-channel and pilot-symbol array-receiver versions, either with conventional or new pilot use, have similar performance at weak Doppler. They also indicate increasing performance gains with increasing Doppler due to the improved use of the pilot information. For a data rate of 144 Kbps with 60 Kmph speed, simulations indicate efficiency gains due to new pilot use of about 25 and 70% in the pilot-channel and pilot-symbol cases, respectively.

I. INTRODUCTION

Optimum exploitation of the pilot signal in wideband CDMA allows capacity gains by coherent detection with power or overhead ratios small enough to reduce interference, but large enough to enable accurate coherent channel identification [1]-[5]. Additional improvements can be achieved if the pilot is just used to resolve the sign ambiguity in blind channel estimation instead of its conventional use for total channel estimation.

In [6] we reported on the analysis and evaluation of both blind and pilot-channel assisted versions of STAR, the spatio-temporal array-receiver [7],[8]. This work allowed us to combine the advantages of these two receiver versions in a hybrid structure that outperforms both in spectrum efficiency while offering substantial savings in the pilot-channel power [9]. Such gains stem from more efficient exploitation of a much weaker pilot, no longer used to identify the channel itself but to resolve the sign ambiguity associated with BPSK-decision-directed blind identification. In [10] we extended use of the hybrid version of STAR to the downlink using pilot channels. Here we show that similar enhancements can be achieved with more efficient use of pilot symbols. We report results of extensive performance evaluation of blind, pilot-channel, and pilot-symbol versions of STAR with both conventional and new pilot use. Additionally, we provide analytical results for optimum values of the channel update step-size and misadjustment previously found by expensive search [6].

II. FORMULATION AND BACKGROUND

A. Data Model

We denote by M the number of the uplink receiving antennas at the base-station and consider a multipath Rayleigh

* Work supported by the Bell/Nortel/NSERC Industrial Research Chair in Personal Communications and by the NSERC Research Grants Program.

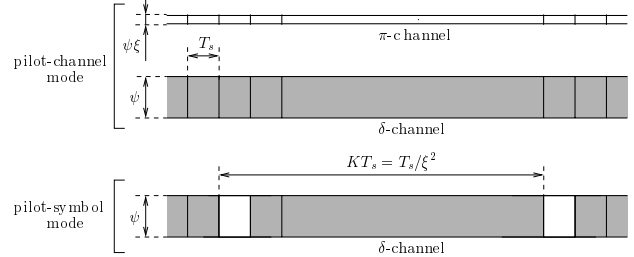


Fig. 1. Pilot modes (data is in grey and pilot is in white).

fading environment with number of paths P and Doppler frequency f_D . After channel coding and interleaving of the information data at the transmitter, the interleaved coded bits are BPSK-modulated at the rate $1/T_s$ where T_s is the symbol duration. The BPSK symbols, denoted as \mathbf{b}_n , where n is the symbol index, may be encoded differentially as $b_n = \mathbf{b}_n \mathbf{b}_{n-1}$. Otherwise, we simply assign $b_n = \mathbf{b}_n$. In either case we spread b_n by a channel code and mark the corresponding data channel with superscript δ . We only use differential encoding jointly with a blind version of STAR (*i.e.*, without a pilot). Otherwise, we either code-multiplex the spread data with a pilot and mark the pilot channel with superscript π or simply insert (*i.e.*, time-multiplex) pilot symbols in the data channel (see Fig. 1). The two pilot structures give rise to pilot-channel and pilot-symbol assisted versions of STAR.

After we despread the data channel at the receiver, we form from the $M \times P$ diversity branches the $MP \times 1$ data observation vector as [9]:

$$\mathbf{Z}_n^\delta = \mathbf{H}_n s_n^\delta + \mathbf{N}_n^\delta = \mathbf{H}_n \psi_n b_n + \mathbf{N}_n^\delta, \quad (1)$$

where $s_n^\delta = \psi_n b_n$ is the data signal component and ψ_n^2 is the total received power. \mathbf{H}_n is the $MP \times 1$ spatio-temporal Rayleigh fading channel vector normalized to \sqrt{M} . \mathbf{N}_n^δ is a space-time uncorrelated Gaussian noise vector with mean zero and variance σ_N^2 after despreading of the data channel. The resulting input SNR after despreading is $SNR_{in} = \psi^2 / \sigma_N^2$ per antenna element.

Similarly when a pilot-channel is used (see Fig. 1), we form the $MP \times 1$ pilot observation vector as [9]:

$$\mathbf{Z}_n^\pi = \mathbf{H}_n s_n^\pi + \mathbf{N}_n^\pi = \mathbf{H}_n \xi \psi_n + \mathbf{N}_n^\pi, \quad (2)$$

where ξ^2 denotes the allocated pilot-to-data power ratio and \mathbf{N}_n^π is a zero-mean space-time uncorrelated Gaussian noise vector with the same variance as \mathbf{N}_n^δ (*i.e.*, σ_N^2).

When a pilot-symbol is used (see Fig. 1), the data sequence b_n is simply assigned a constant “1” once every K symbols, although insertion of pilot blocks is possible. Hence we have $b_{n'K} = 1$ and $s_{n'K}^\delta = s_{n'K}^\delta = \psi_{n'K}$. In this case, $\xi^2 = 1/K$ denotes the allocated pilot-to-data overhead ratio.

In the following, we investigate the five versions of STAR summarized in Tab. 1. We give a brief overview of the first three structures of STAR studied in [9] before we introduce the two additional pilot-symbol assisted versions.

B. Rx1: Blind STAR

The blind version of STAR, denoted by Rx1 (see Tab. 1), does not need a pilot. First, it uses the channel estimate $\hat{\mathbf{H}}_n$ at iteration n to extract the data signal component by spatio-temporal MRC [6],[9]:

$$\hat{s}_n^\delta = \text{Re} \left\{ \hat{\mathbf{H}}_n^H \mathbf{Z}_n^\delta / M \right\}. \quad (3)$$

The data sequence b_n is then estimated as $\hat{b}_n = \text{Sign} \{ \hat{s}_n^\delta \}$.

In a second step, Rx1 feeds back the estimate of the data signal component \hat{s}_n^δ (or $\hat{\psi}_n \hat{b}_n$)¹ in a decision feedback identification (DFI) scheme to update the channel estimate as follows [6],[9]:

$$\hat{\mathbf{H}}_{n+1} = \hat{\mathbf{H}}_n + \mu \left(\mathbf{Z}_n^\delta - \hat{\mathbf{H}}_n \hat{s}_n^\delta \right) \hat{s}_n^\delta, \quad (4)$$

where $\hat{\mathbf{H}}_n$ is the adaptive channel estimate and μ the adaptation step-size.

The simple decision feedback identification (DFI) scheme [6] of Eqs. (3) and (4) identifies the channel within a sign ambiguity, say $a = \pm 1$, thereby giving $\hat{\mathbf{H}}_n \simeq a \mathbf{H}_n$, $\hat{s}_n^\delta \simeq a \psi_n b_n$, and $\hat{b}_n = \text{Sign} \{ \hat{s}_n^\delta \} \simeq a b_n$. However, differential decoding of the hard decisions \hat{b}_n resolves the sign ambiguity in the BPSK symbol estimates $\hat{b}_n = \hat{b}_n \hat{b}_{n-1} = \text{Sign} \{ \hat{s}_n^\delta \hat{s}_{n-1}^\delta \}$. These values can be passed on to the channel decoder after deinterleaving. For better performance, Rx1 transmits instead the differential soft output $\hat{s}_n^\delta = \hat{s}_n^\delta \hat{s}_{n-1}^\delta$.

C. Rx2: STAR with Conventional Pilot-Channel

The second version of STAR, denoted by Rx2 (see Tab. 1), uses a pilot-channel [3],[5] for conventional channel identification². Rx2 also extracts the signal component estimate \hat{s}_n^δ using Eq. (3). However, it exploits the fact that the pilot signal is a known reference signal (*a priori* constant “1”) and modifies the DFI scheme of Rx1 in Eqs. (3) and (4) as follows [9]. Rx2 extracts the pilot signal component estimate:

$$\hat{s}_n^\pi = \text{Re} \left\{ \hat{\mathbf{H}}_n^H \mathbf{Z}_n^\pi / M \right\}, \quad (5)$$

then feeds it back³ to the following channel identification procedure:

$$\hat{\mathbf{H}}_{n+1} = \hat{\mathbf{H}}_n + \mu \left(\mathbf{Z}_n^\pi - \hat{\mathbf{H}}_n \hat{s}_n^\pi \right) \hat{s}_n^\pi. \quad (6)$$

¹For lack of space, the steps that estimate the received power ψ_n^2 for power control and for decision feedback can be found in [9].

²Note that conventional reference-assisted techniques estimate each diversity finger with a multiple-tap low-pass filter [1]-[5]. With less computations here, we identify each finger with an optimized single-tap adaptive-filter using the DFI procedure of Eq. (6) in the pilot-channel case or Eq. (9) in the pilot-symbol case.

³We actually feed back $\xi \hat{\psi}_n$ (or $|\hat{s}_n^\pi|$) with the *a priori* known positive sign of the pilot. Note that the DFI step of Eq. (6) could be updated at a slower rate if the pilot signal is transmitted in short bursts on the pilot channel. Extension in this case is *ad hoc*.

	pilot mode	pilot use
Rx1	none	none (<i>i.e.</i> , blind without pilot)
Rx2	pilot-channel	channel identification (<i>i.e.</i> , conventional)
Rx3	pilot-channel	ambiguity resolution (<i>i.e.</i> , enhanced)
Rx4	pilot-symbol	channel identification (<i>i.e.</i> , conventional)
Rx5	pilot-symbol	ambiguity resolution (<i>i.e.</i> , enhanced)

Tab. 1. Description of the tested versions of STAR.

As a result, the DFI scheme identifies the channel without ambiguity (*i.e.*, $a = 1$). Hence, Rx2 estimates the BPSK symbol estimates as $\hat{b}_n = \hat{b}_n = \text{Sign} \{ \hat{s}_n^\delta \}$. These values can be passed on to the channel decoder after deinterleaving. For better performance, Rx2 transmits instead the soft output $\hat{s}_n^\delta = \hat{s}_n^\delta$.

D. Rx3: STAR with Enhanced Pilot-Channel

The third version of STAR, denoted by Rx3 (see Tab. 1), is a hybrid of Rx1 and Rx2. Like Rx1, it applies the blind DFI procedure of Eqs. (3) and (4) to estimate the channel within a sign ambiguity denoted a . Like Rx2, it uses a pilot-channel. However, with much weaker power it exploits the pilot more efficiently to accurately estimate then resolve the sign ambiguity of a [9]. Noticing that the pilot signal component $\hat{s}_n^\pi \simeq a \psi_n \xi$ carries a noisy value of a , Rx3 estimates it by taking the sign of \hat{s}_n^π after averaging over consecutive blocks of A samples, giving for $n \in \{n'A, \dots, (n'+1)A - 1\}$:

$$\bar{s}_n^\pi = \sum_{i=0}^{A-1} \hat{s}_{n'+A+i}^\pi / A, \quad (7)$$

$$\hat{a}_n = \text{Sign} \{ \bar{s}_n^\pi \}. \quad (8)$$

The averaging step above enables accurate estimation of a with a much weaker pilot power [9]. Hence, Rx3 estimates the BPSK symbol estimates as $\hat{b}_n = \hat{a}_n \hat{b}_n = \text{Sign} \{ \hat{a}_n \hat{s}_n^\delta \}$. These values can be passed on to the channel decoder after deinterleaving. For better performance, Rx3 transmits instead the soft output $\hat{s}_n^\delta = \hat{a}_n \hat{s}_n^\delta$.

In [9] we showed both by analysis and simulations that Rx3 outperforms Rx2 in capacity and spectrum efficiency while offering substantial savings in the pilot-channel power. Such gains stem from more efficient exploitation of a much weaker pilot, no longer used to identify the channel itself but to resolve the sign ambiguity it carries with blind identification. The question we address below is whether similar enhancements can be achieved with more efficient use of pilot-symbols.

III. NEW PILOT-SYMBOL VERSIONS OF STAR

In the following, we introduce two additional pilot-symbol assisted structures of STAR which are counterparts of pilot-channel assisted versions Rx2 and Rx3, respectively. Later we show by analysis and simulations that each of these two additional pilot-symbol versions performs nearly as well as its pilot-channel assisted counterpart. With either pilot-mode, however, the new scheme allows substantial savings in power or overhead and significant gains in spectrum efficiency over the conventional one.

A. Rx4: STAR with Conventional Pilot-Symbol

The fourth version of STAR, denoted by Rx4 (see Tab. 1), uses pilot symbols for conventional channel identification [1],[2],[4],[5] (see footnote 2). Its DFI procedure is similar to that of Rx1 and Rx3 in that it combines Eqs. (3) and (4). However, it only feeds back the signal components containing the pilot symbols inserted in the data sequence once every K symbols:

$$\hat{\mathbf{H}}_{(n'+1)K} = \hat{\mathbf{H}}_{n'K} + \mu \left(\mathbf{Z}_{n'K}^\delta - \hat{\mathbf{H}}_{n'K} \hat{s}_{n'K}^\pi \right) \hat{s}_{n'K}^\pi, \quad (9)$$

where $\hat{s}_{n'K}^\pi = \hat{\psi}_{n'K}$. Similarly to Rx2, the DFI scheme of Rx4 identifies the channel without ambiguity (*i.e.*, $a = 1$) and allows estimation of $\hat{\mathbf{b}}_n$ and \hat{s}_n^δ using the same hard and soft decision rules, respectively.

Notice, however, that Rx4 updates the DFI procedure less frequently than Rx2, namely at the pilot-symbol rate $1/KT_s$. On the one hand, the channel subsampled at the DFI-update instants appears to vary K times faster with a relative normalized Doppler $Kf_D T_s$. Channel identification errors are expected to increase with faster time-variations [9]. On the other hand, the power of the feedback signal in Rx4, $|\hat{s}_{n'K}^\pi|^2 = \hat{\psi}_{n'K}^2$, is K times stronger than in Rx2 where $|\hat{s}_n^\pi|^2 = \xi^2 \hat{\psi}_n^2 = \hat{\psi}_n^2/K$. Channel identification errors are expected to decrease with stronger feedback signals [9]. Later we show a non-trivial analytical result that the corresponding loss and gain in channel identification errors balance each other. The minimum channel misadjustment achievable remains constant if we increase both the relative Doppler and the feedback-signal's power by the same factor K . We actually show that Rx2 and Rx4 identify the channel equally well.

B. Rx5: STAR with Enhanced Pilot-Symbol

Similarly to Rx3, the fifth version of STAR denoted by Rx5 (see Tab. 1) is a hybrid of Rx1 and Rx4. It applies the blind DFI procedure of Eqs. (3) and (4) to estimate the channel within a sign ambiguity denoted a . However, it uses a pilot-symbol to estimate then resolve the sign ambiguity a . Assume for simplicity that a block of A consecutive symbols contains exactly Q pilot symbols (*i.e.*, $A = QK$). Rx4 modifies Eqs. (7) simply by averaging the pilot signal component estimate over these Q symbols for $n \in \{n'A, \dots, (n'+1)A - 1\}$:

$$\bar{s}_n^\pi = \sum_{i=0}^{Q-1} \hat{s}_{n'A+Ki}^\pi / Q. \quad (10)$$

before taking its sign as in Eq. (8). Similarly to Rx3, Rx5 thereby resolves the sign ambiguity and hence estimates $\hat{\mathbf{b}}_n$ and \hat{s}_n^δ using the same hard and soft decision rules, respectively.

Notice that Rx5 in Eq. (10) estimates the pilot-signal component from $K = A/Q$ fewer values than Rx3 in Eq. (7). The variance of the residual noise present in \bar{s}_n^π is thereby increased by factor K . However, bear in mind that the pilot-signal power in Rx5 is K times stronger than in Rx3. The SNR of \bar{s}_n^π before sign ambiguity estimation in Eq. (8) is therefore the same for both receiver versions. Despite the differences between Rx3 and Rx5, the sign-estimation step in Eq. (7) or

1. initialize capacity $C = 0$.
2. start computation loop:
 - 2.1. increment capacity $C = C + 1$,
 - 2.2. noise variance is $\sigma_N^2 = C\nu^2(1 + \eta^2)/L$,
 - 2.3. misadjustment is $\beta^2(\mu, \sigma_N^2, f_D T_s)$,
 - 2.4. compute BER:
 - 2.4.1 compute data output SNR $E[|s_n^\delta|^2/|\hat{s}_n^\delta - s_n^\delta|^2]$
 $SNR_{\text{out}}^\delta = SNR_{\text{in}} \times M/[1 + (P + SNR_{\text{in}})\beta^2]$,
 - 2.4.2 $p_e^\delta = P(\{\hat{b}_n \neq b_n\}) = \frac{1}{2} \text{erfc}(\sqrt{SNR_{\text{out}}^\delta})$,
 - 2.4.3 $p_e = P(\{\hat{\mathbf{b}}_n \neq \mathbf{b}_n\}) = 2 p_e^\delta (1 - p_e^\delta)$,
 - 2.5. if $p_e \leq P_e$ goto 2.1, else exit loop.
3. decrement capacity $C = C - 1$.

Fig. 2. Procedure computing capacity $C^1(P_e, \mu)$ of Rx1 at a given fading rate $f_D T_s$.

1. initialize capacity $C = 0$.
2. start computation loop:
 - 2.1. increment capacity $C = C + 1$,
 - 2.2. if Rx2, noise variance is $\sigma_N^2 = C\nu^2(1 + \xi^2)(1 + \eta^2)/L$,
if Rx4, noise variance is $\sigma_N^2 = C\nu^2(1 + \eta^2)/L$,
 - 2.3. if Rx2, misadjustment is $\beta^2(\mu\xi^2, \sigma_N^2/\xi^2, f_D T_s)$,
if Rx4, misadjustment is $\beta^2(\mu\xi^2, \sigma_N^2, f_D T_s/\xi^2)$,
 - 2.4. compute BER:
 - 2.4.1 data output SNR $E[|s_n^\delta|^2/|\hat{s}_n^\delta - s_n^\delta|^2]$ is
 $SNR_{\text{out}}^\delta = SNR_{\text{in}} \times M/[1 + (P + SNR_{\text{in}})\beta^2]$,
 - 2.4.2 $p_e = P(\{\hat{b}_n \neq b_n\}) = \frac{1}{2} \text{erfc}(\sqrt{SNR_{\text{out}}^\delta})$,
 - 2.5. if $p_e \leq P_e$ goto 2.1, else exit loop.
3. decrement capacity $C = C - 1$.

Fig. 3. Procedure computing capacity $C^2(P_e, \mu, \xi^2)$ of Rx2 or $C^4(P_e, \mu, \xi^2)$ of Rx4 at a given fading rate $f_D T_s$.

(10) results in the same sign estimation error. Hence we easily show in the following analysis section that Rx3 and Rx5 have equivalent performance.

IV. NEW ANALYTICAL RESULTS

In [9], we proposed simple computation procedures to evaluate and optimize the uplink capacity C in terms of the number of users per cell for Rx1, Rx2, and Rx3. These procedures are shown in Figs. 2, 3 and 4. Here, we derive two additional computation procedures for the pilot-symbol assisted versions of STAR, namely Rx4 and Rx5. For lack of space, we show these procedures on the same figures as Rx2 and Rx4, respectively. As a brief reminder of some of the parameters that appear in these procedures, L denotes the processing gain, η^2 takes into account the outcell-to-incell interference ratio, ν^2 takes into account the effect of time-delay mismatch between shaping pulses, the speech or data transmission activity factor denoted as p_{Tx} , and the outage probability [11], and β^2 denotes the channel identification misadjustment or mean square error (*i.e.*, $E[\|\hat{\mathbf{H}}_n - \mathbf{H}_n\|^2]/MP$) [6],[9].

For a specified maximum BER value before channel decoding, say P_e (*i.e.*, quality of service), these procedures allow optimization of the capacity $C(P_e, \mu, \xi^2)$ with respect to the step-size μ and the pilot-to-data power ratio ξ^2 (for details see [6],[9]). In the case of pilot-symbols, the pilot-to-data overhead ratio ξ^2 must be optimized by maximizing the spectrum efficiency defined as:

$$\mathcal{E}(P_e, \mu, \xi^2) = \frac{C p_{\text{Tx}} r_c}{L}, \quad (11)$$

1. initialize capacity $C = 0$.
2. start computation loop:
 - 2.1. increment capacity $C = C + 1$,
 - 2.2. if Rx3, noise variance is $\sigma_N^2 = C\nu^2(1 + \xi^2)(1 + \eta^2)/L$,
if Rx5, noise variance is $\sigma_N^2 = C\nu^2(1 + \eta^2)/L$,
 - 2.3. misadjustment is $\beta^2(\mu, \sigma_N^2, f_D T_s)$,
 - 2.4. compute BER:
 - 2.4.1 data output SNR $E[|s_n^\delta|^2/|\hat{s}_n^\delta - s_n^\delta|^2]$ is
 $SNR_{out}^\delta = SNR_{in} \times M/[1 + (P + SNR_{in})\beta^2]$,
 - 2.4.2 if Rx3, pilot output SNR $E[|s_n^\pi|^2/|\hat{s}_n^\pi - s_n^\pi|^2]$ is
 $SNR_{out}^\pi = \xi^2 SNR_{out}^\delta$,
if Rx5, pilot output SNR is
 $SNR_{out}^\pi = SNR_{out}^\delta$,
 - 2.4.3 $p_e^\delta = P(\{\hat{b}_n \neq b_n\}) = \frac{1}{2} \operatorname{erfc}(\sqrt{SNR_{out}^\delta})$,
 - 2.4.4 if Rx3, $p_e^\pi = P(\{\hat{a}_n \neq a\}) = \frac{1}{2} \operatorname{erfc}(\sqrt{A SNR_{out}^\pi})$,
if Rx5, $p_e^\pi = \frac{1}{2} \operatorname{erfc}(\sqrt{A \xi^2 SNR_{out}^\pi})$,
 - 2.4.5 $p_e = P(\{\hat{\mathbf{b}}_n \neq \mathbf{b}_n\}) = p_e^\sigma(1 - p_e^\delta) + p_e^\delta(1 - p_e^\sigma)$,
 - 2.5. if $p_e \leq P_e$ goto 2.1, else exit loop.
3. decrement capacity $C = C - 1$.

Fig. 4. Procedure computing capacity $C^3(P_e, \mu, \xi^2)$ of Rx3 or $C^5(P_e, \mu, \xi^2)$ of Rx5 at a given fading rate $f_D T_s$.

for the pilot-channel versions and:

$$\mathcal{E}(P_e, \mu, \xi^2) = \frac{C(1 - \xi^2) p_{Tx} r_c}{L} \simeq \frac{C p_{Tx} r_c}{(1 + \xi^2)L}, \quad (12)$$

for the pilot-symbol versions (assuming $\xi^2 \ll 1$ in low-to-medium normalized Doppler $f_D T_s$, see simulations in section V-B). p_{Tx} is the speech/data transmission activity factor and r_c is the channel coding rate. In contrast to pilot-channel versions where maximization of capacity over ξ^2 optimizes efficiency, increase in the pilot overhead ratio ξ^2 will always improve identification and capacity while reducing efficiency. Optimum values to find for ξ^2 are hence those which directly maximize efficiency.

For lack of space, we do not provide optimum performance results by analytical computation. They match closely those obtained by simulations in the next section. We provide instead new interesting analytical results that establish an equivalence in performance between the two pilot-channel versions of STAR and their two pilot-symbol counterparts, respectively.

In previous work we only suggested minimization of the misadjustment β^2 by search over the optimal step-size within given bounds [9]. Here we provide non-trivial analytical expressions both for the optimal step-size and the resulting minimum misadjustment and time constant (not necessarily the smallest) as (see details in [13]):

$$\mu_{opt} \simeq 2 \left[(\pi f_D T_s) / (\sqrt{P} \psi^2 \sigma_N) \right]^{2/3}, \quad (13)$$

$$\beta_{min}^2 = \frac{3}{2} \left[(\pi f_D T_s) / (\sqrt{P} SNR_{in}) \right]^{2/3}, \quad (14)$$

$$\tau_{opt} \simeq \frac{1}{4} \left[\sqrt{P} / (\pi f_D T_s \sqrt{SNR_{in}}) \right]^{\frac{2}{3}}. \quad (15)$$

As shown in Fig. 5-a, theoretical values for misadjustment derived from Eq. (14) show a very good fit to those obtained by simulations. In Fig. Fig. 5-b, theoretical values for optimal step-size in Eq. (13) also match very well with the values obtained by search then validated by simulations in [6]. They

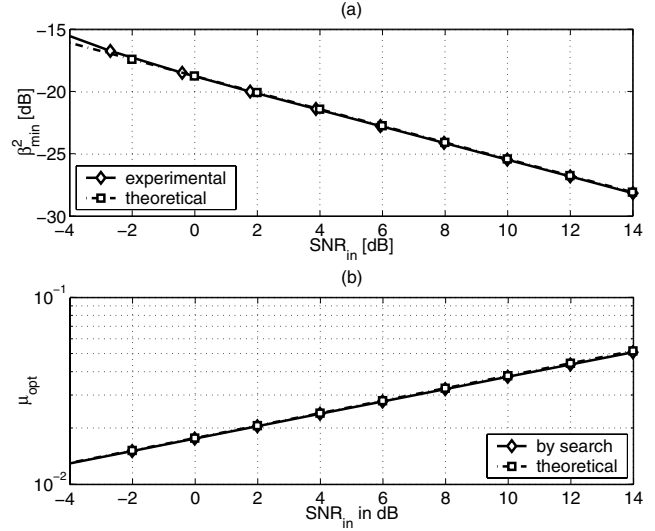


Fig. 5. (a): minimum misadjustment in dB vs. SNR in dB with optimum step-size μ_{opt} of Eq. (13), (b): optimum step-size μ_{opt} vs. SNR in dB for the low-rate/low-speed setup of section V-A with $M = 4$ antennas.

reduce computational complexity and allow huge savings in processing time.

To the best of our knowledge, these expressions (which apply to both blind and reference-assisted receivers [6]) are the first to provide practical means for optimal tuning of adaptive channel identification and for prediction of step-size, misadjustment and convergence time in a multipath Rayleigh fading environment.

Furthermore, the new analytical results suggest that pilot-channel and pilot-symbol versions of STAR, with either conventional or enhanced pilot use, require the same optimum step-size and convergence time and result in the same misadjustment when operating with the same pilot power and overhead fractions, respectively. The proof is easy to establish with simple updates of the theoretical expressions of Eqs. (13) to (15) (see details in [13]).

Here we simply validate this result at the link-level by comparing the BER (*i.e.*, $P(\{\hat{b}_n \neq b_n\})$). Curves in Fig. 6 first indicate that more efficient exploitation of pilot channels or symbols for only phase-ambiguity resolution outperforms their conventional use for channel-identification. The receiver versions with enhanced pilot use (*i.e.*, Rx3 and Rx5) perform practically the same with 1 or 5% fractions of the pilot power or overhead thereby showing that long-term averaging in Eqs. (7) and (10) indeed significantly reduces phase ambiguity estimation errors in Eq. (8) from very weak pilot signals. On the other hand, the receiver versions with conventional pilot use (*i.e.*, Rx2 and Rx4) see their performance drop when the pilot power or overhead fraction is reduced by half from 10 to 5%. Simulations actually indicate that Rx2 and Rx4 with 10% fraction perform worse than Rx3 and Rx5 with 1% fraction only. The curves in Fig. 6 also suggest that pilot-channel and pilot-symbol versions, with either conventional or enhanced pilot use, perform similarly thereby confirming our analytical assertions at the link-level. Below we extend the scope of our assertions to the system-level with focus on

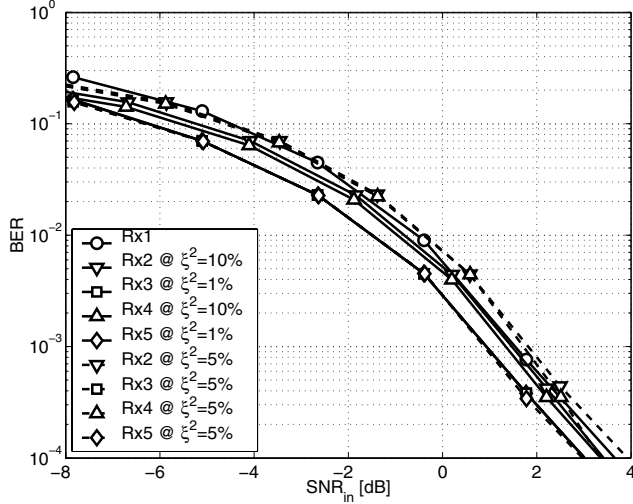


Fig. 6. BER vs. SNR in dB for different versions of STAR (see Tab. 1) with optimum step-size μ_{opt} of Eq. (13) (for the low-rate/low-speed setup of section V-A with $M = 4$ antennas).

spectrum efficiency.

The expression for misadjustment in Eq. (14) suggests that multiplying the noise variance σ_N^2 or the normalized Doppler $f_D T_s$ by factor $1/\xi^2$ in computation step 2.3 of Fig. 3 yields the same misadjustment β_{min}^2 for Rx2 and Rx4, respectively. Taking into account the fact that expressions for σ_N^2 in step 2.2 must be equated for Rx2 and Rx4 in order to achieve the same target BER P_e in step 2.4, we should find after optimization:

$$C^2(P_e, \mu_{\text{opt}}, \xi_{\text{opt}}^2)(1 + \xi_{\text{opt}}^2) \simeq C^4(P_e, \mu_{\text{opt}}, \xi_{\text{opt}}^2). \quad (16)$$

Hence exploiting Eqs. (11) and (12) we show that:

$$\mathcal{E}^2(P_e, \mu_{\text{opt}}, \xi_{\text{opt}}^2) \simeq \mathcal{E}^4(P_e, \mu_{\text{opt}}, \xi_{\text{opt}}^2). \quad (17)$$

With the same optimal parameters, analysis suggests that Rx2 and Rx4 achieve the same maximum spectrum efficiency performance at low-to-medium Doppler (where approximation in Eq. (12) holds).

This equivalence is easier to establish for the versions of STAR with enhanced pilot use. In step 2.4.2 of Fig. 4, SNR_{out}^{π} in Rx3 is weaker than in Rx5 by factor ξ^2 . However, this factor is considered in Rx5 when computing the error probability p_e^{σ} over a in step 2.4.4 of Fig. 4. Similarly from step 2.2 of Fig. 4, we find $C^3(P_e, \mu_{\text{opt}}, \xi_{\text{opt}}^2)(1 + \xi_{\text{opt}}^2) \simeq C^5(P_e, \mu_{\text{opt}}, \xi_{\text{opt}}^2)$ and hence show that $\mathcal{E}^3(P_e, \mu_{\text{opt}}, \xi_{\text{opt}}^2) \simeq \mathcal{E}^5(P_e, \mu_{\text{opt}}, \xi_{\text{opt}}^2)$ after optimization.

A similar conclusion regarding the equivalence between conventional pilot-channel and pilot-symbol reference-assisted receivers was reached in [5] at the link-level based on expressions for misadjustment of channel estimation with low-pass filtering (see footnote 2). Here we establish an equivalence between pilot-channel and pilot-symbol receivers in both cases of conventional pilot use for channel identification and enhanced pilot use for sign ambiguity resolution in terms of misadjustment, optimum step-size, time-constant, and required SNR (or BER) at the link-level; and in terms of spectrum efficiency at the system-level (in the low-to-medium Doppler case) as validated next by simulations.

(a): 144 Kbps @ 10^{-5} - 1 Km/h $\rightarrow f_D^0 T_s^0$

	Rx1	Rx2	Rx3	Rx4	Rx5
μ_{opt}	0.001	0.006	0.001	0.050	0.001
ξ_{opt}^2 [%]	0	2.5	0.6	1.0	1.0
SNR_{req} [dB]	0.71	-2.30	-2.49	-2.47	-2.66
C [users/cell]	5	12	13	13	14
\mathcal{E} [bps/Hz/2]	0.078	0.188	0.203	0.201	0.217

(b): 9.6 Kbps @ 10^{-3} - 1 Km/h $\rightarrow 15 \times f_D^0 T_s^0$

	Rx1	Rx2	Rx3	Rx4	Rx5
μ_{opt}	0.005	0.032	0.008	0.040	0.004
ξ_{opt}^2 [%]	0	10.0	1.0	4.2	1.0
SNR_{req} [dB]	-0.94	-3.16	-3.47	-3.31	-3.51
C [users/cell]	448	711	819	732	843
\mathcal{E} [bps/Hz/2]	0.197	0.312	0.356	0.308	0.366

(c): 144 Kbps @ 10^{-5} - 60 Km/h $\rightarrow 60 \times f_D^0 T_s^0$

	Rx1	Rx2	Rx3	Rx4	Rx5
μ_{opt}	0.010	0.079	0.079	0.126	0.063
ξ_{opt}^2 [%]	0	39.8	0.6	33.3	8.3
SNR_{req} [dB]	4.03	1.29	1.08	1.13	1.20
C [users/cell]	1	4	5	4	5
\mathcal{E} [bps/Hz/2]	0.016	0.063	0.078	0.042	0.072

(d): 9.6 Kbps @ 10^{-3} - 60 Km/h $\rightarrow 60 \times 15 \times f_D^0 T_s^0$

	Rx1	Rx2	Rx3	Rx4	Rx5
μ_{opt}	0.126	0.126	0.126	0.200	0.167
ξ_{opt}^2 [%]	0	63.1	63.1	33.3	16.7
SNR_{req} [dB]	0.71	-1.34	0.28	-2.28	0.57
C [users/cell]	288	375	251	382	308
\mathcal{E} [bps/Hz/2]	0.127	0.165	0.110	0.112	0.113

Tab. 2. Receivers' performance results with two receive antennas in 5 MHz bandwidth for (a): data calls with slow mobility, (b): voice calls with slow mobility, (c): data calls with high mobility, (d): voice calls with high mobility (spectrum efficiency, lower @ 10^{-5} than @ 10^{-3} , is per antenna).

V. SYSTEM-LEVEL PERFORMANCE EVALUATION

A. Simulation Setup

We consider a wideband CDMA system with 5 MHz bandwidth, $M = 2$ receive antennas and $P = 3$ equal-power paths. The mobile has two possible speeds of 1 and 60 Km/h corresponding, respectively, to Doppler shifts f_D of about 1.8 and 105.6 Hz at a carrier frequency of 1.9 GHz. Power control (PC) requests an incremental change of ± 0.25 dB in transmitted power every 0.625 ms with a delay of 0.625 ms and an error of 10% over the PC bit command. The user information is encoded using a convolutional code with rate $r_c = 1/2$ and constraint length of 9. We consider a data rate of 144 Kbps with processing gain $L = 16$ and a voice rate of 9.6 Kbps with processing gain $L = 256$. The target BER after channel decoding is 10^{-5} and 10^{-3} for the 144 and 9.6 Kbps rates, respectively, while the activity factor p_{Tx} is 100% and 45%, respectively. We use the simulation tool proposed in [11] to optimize spectrum efficiency by grid search over μ and ξ^2 , a time consuming task.

B. Simulation Results

Simulations again indicate that more efficient exploitation of pilot channels or symbols for only sign-ambiguity resolution

outperforms their conventional use for channel-identification (*i.e.*, $Rx3 > Rx2$ and $Rx5 > Rx4$) for a range of normalized Doppler values shown in Tab. 2. They also suggest that pilot-channel and pilot-symbol versions, with either conventional or new pilot use, perform nearly the same at low-to-medium Doppler, thereby confirming again our analysis assertions (*i.e.*, $Rx2 \simeq Rx4$ and $Rx3 \simeq Rx5$).

For low and medium Doppler in Tabs. 2-a and 2-b, efficiency gains due to new pilot use are in the range of 10% and 15-20%, respectively. In the pilot-channel case, pilot power savings which prolong battery life are in the range of 75% for low Doppler and 90% for medium Doppler. For high Doppler in Tab. 2-c, efficiency gains due to the improved use of the pilot jump to 25 and 70% in the pilot-channel and pilot-symbol cases, respectively, while power savings jump up to about 98% in the pilot-channel case. In the pilot-symbol case, overhead savings with no other benefits than those already accounted for in spectrum efficiency gains jump from 0% at low Doppler (see Tab. 2-a) to about 75% at both medium and high Doppler (see Tabs. 2-b and 2-c).

Asymptotically, all pilot-aided versions of STAR perform the same with perfect channel estimation [6]. As channel estimation conditions worsen from low to high Doppler, gains in spectrum efficiency of $Rx3$ and $Rx5$ over $Rx2$ and $Rx4$, respectively, increase as well as do savings in pilot power or overhead. At the same time, the gap in performance between $Rx2$ and $Rx4$ and between $Rx3$ and $Rx5$ widens, thereby showing the limitations of the previous analytical results (*i.e.*, $Rx2 \simeq Rx4$ and $Rx3 \simeq Rx5$).

In the very high range of $f_D T_s$ in Tab. 2-d, *i.e.*, about 1000 times the low reference range $f_D^0 T_s^0$ in Tab. 2-a, predictions no longer hold. Here, the conventional pilot-channel version $Rx2$ performs best. The conventional pilot-symbol version $Rx4$ sees even higher Doppler with slower identification update at the pilot-symbol rate and hence performs worse. Use of pilots for sign ambiguity resolution suffers from more severe sign error propagation due to more frequent ambiguity hops when tracking faster channels. Hence $Rx5$ and $Rx3$ perform nearly as well as $Rx4$ and worse than $Rx2$. Limiting the impact of sign ambiguity hops in $Rx3$ and $Rx5$ is an issue we intend to address in the future. Finally, it is worth noting that the less complex blind version $Rx1$ shows relatively stronger robustness to faster channel time-variations [6],[9] and falls second in performance.

VI. DISCUSSION AND CONCLUSIONS

For a wide range of normalized Doppler values both in the low to high range, both analysis and simulations indicate that exploitation of pilots in CDMA array-receivers for simple sign-ambiguity resolution only allows significant efficiency gains as well as power or overhead savings over the same array-receiver versions which use pilots for conventional channel identification only. They also suggest that pilot-channel and pilot-symbol array-receiver versions, either with conventional or new pilot-use, have equivalent performance.

Pilot-symbol versions are, however, more sensitive to very high values of the normalized Doppler. Besides, they need

more careful design of pilot insertion schemes before interleaving (*e.g.*, S-Random). On the other hand, pilot-channels may require additional despreading operations with a higher computational cost. They also need more careful design of interference suppression constraints in a multiuser detection framework [12].

Standards already provide recommendations for conventional use of pilots for both the uplink and the downlink. However, the more efficient use of pilots suggested here for enhanced performance of wideband CDMA array-receivers, beyond the minor modifications required, is standard-compliant. It applies to the uplink with BPSK, but can be easily extended to the downlink [10] and/or to higher-order modulations [13].

REFERENCES

- [1] J.K. Cavers, "An analysis of pilot symbol assisted modulation for Rayleigh fading channels", *IEEE Trans. Vehic. Tech.*, vol. 40, no. 4, pp. 686-693, November 1991.
- [2] C. D'Armours, M. Moher, and A. Yongacoglu, "Comparison of pilot-symbol assisted and differentially detected BPSK for DS-SS systems employing RAKE receivers in Rayleigh fading channels", *IEEE Trans. Vehic. Tech.*, vol. 47, no. 4, pp. 1258-1267, November 1997.
- [3] P. Schramm, "Analysis and optimization of pilot-channel-assisted BPSK for DS-SS systems", *IEEE Trans. Comm.*, vol. 46, no. 9, pp. 1122-1124, September 1998.
- [4] P. Schramm, "Pilot symbol assisted BPSK on Rayleigh fading channels with diversity: performance analysis and parameter optimization", *IEEE Trans. Comm.*, vol. 46, no. 12, pp. 1560-1563, December 1998.
- [5] F. Ling, "Optimal reception, performance bound, and cutoff rate analysis of reference-assisted coherent CDMA communications with applications", *IEEE Trans. Comm.*, vol. 47, no. 10, pp.1583-1592, October 1999.
- [6] S. Affes and P. Mermelstein, "Comparison of pilot-assisted and blind CDMA array-receivers adaptive to Rayleigh fading rates", *Proc. of IEEE PIMRC'99*, 1999, vol. 3, pp. 1186-1192.
- [7] S. Affes and P. Mermelstein, "A new receiver structure for asynchronous CDMA: STAR - The spatio-temporal array-receiver", *IEEE J. Sel. Areas Comm.*, vol. 16, no. 8, pp. 1411-1422, October 1998.
- [8] K. Cheikhrouhou, S. Affes, and P. Mermelstein, "Impact of synchronization on performance of enhanced array-receivers in wideband CDMA networks", *IEEE J. Sel. Areas Comm.*, vol. 19, no. 12, pp. 2462-2476, December 2001.
- [9] S. Affes, A. Louzi, N. Kandil, and P. Mermelstein, "A high capacity CDMA array-receiver requiring reduced pilot power", *Proc. of IEEE GLOBECOM'2000*, 2000, vol. 2, pp. 910-916.
- [10] S. Affes, A. Saadi, and P. Mermelstein, "Pilot-assisted STAR for increased capacity and coverage on the downlink of wideband CDMA networks", *Proc. of IEEE SPAWC'01*, 2001, pp. 310-313.
- [11] A. Jalali and P. Mermelstein, "Effects of diversity, power control, and bandwidth on the capacity of microcellular CDMA systems", *IEEE J. Sel. Areas Comm.*, vol. 12, no. 5, pp. 952-961, June 1994.
- [12] Affes, H. Hansen, and P. Mermelstein, "Interference subspace rejection: A framework for multiuser detection in wideband CDMA", *IEEE J. Sel. Areas Comm.*, vol. 20, no. 2, pp. 287-302, February 2002.
- [13] S. Affes and P. Mermelstein, "Adaptive S space-time processing for wireless CDMA", in *Adaptive Signal Processing: Application to Real-World Problems*, J. Benesty and A.H. Huang, Eds., Springer, Berlin, to appear, February 2003.